Cavity implementation of quantum interference in a Λ-type atom

Peng Zhou*
School of Physics, Georgia Institute of Technology, Atlanta, Georgia 30332-0430
and Department of Physics, Hunan Normal University, Changsha 410081, China
(Received 13 September 2000; published 12 January 2001)

A scheme for engineering quantum interference in a Λ-type atom coupled to a frequency-tunable, single-mode cavity field with a preselected polarization at finite temperature is proposed. Interference-assisted population trapping, population inversions, and probe gain at one sideband of the Autler-Townes spectrum are predicted for certain cavity resonant frequencies.

DOI: 10.1103/PhysRevA.63.023810 PACS number(s): 42.50.Gy, 03.65.−w, 32.80.−t, 42.50.Ct

Within recent years, there has been a resurgence of interest in the phenomenon of quantum interference between different transition paths of atoms [1]. The principal reason is that it lies at the heart of many new effects and applications of quantum optics, such as lasing without population inversion [2], electromagnetically induced transparency [3], enhancement of the index of refraction without absorption [4], fluorescence quenching [5–7], and spectral line narrowing [7,8].

The basic system consists of a singlet state connected to a closely spaced doublet by a single electromagnetic vacuum interaction [6,7,9], so that the two transition pathways from the doublet states to the singlet are not independent and may interfere. It is important for these effects that the dipole moments of the transitions involved are parallel, so that the cross-transition terms are maximal. From the experimental point view, however, it is difficult to find isolated atomic systems which have parallel moments [2,6,9–11].

Various alternative proposals [3,8,10,13] have been made for generating quantum interference effects. For example, for three-level atomic systems (in *V*, Λ, and Ξ configurations) excited by two laser fields: one being a strong pump field to drive two levels (say $|1\rangle$ and $|2\rangle$) and the other being a weak probe field at different frequency to probe the levels $|0\rangle$ and $|1\rangle$ or $|2\rangle$, the strong coherent field can drive the levels $|1\rangle$ and $|2\rangle$ into superpositions of these states, so that different atomic transitions are correlated. For such systems, the cross-transition terms are evident in the atomic dressed picture [3,8,13]. Other schemes for generating quantum interference, based on cavity QED, have been also proposed [10]. In fact, the experimental observation of the interference-induced suppression of spontaneous emission was carried out in sodium dimers where the excited sublevels are superpositions of singlet and triplet states that are mixed by a spin-orbit interaction [5]. Detailed theoretical investigations of this system have recently been provided [11,12].

The major purpose of this paper is to propose a scheme whereby quantum interference can be readily engendered in realistic practical situations. We study a Λ-type atom coupled to a frequency-tunable single-mode cavity field with a preselected polarization which is damped by a thermal reservoir, and show that maximal quantum interference (equivalently, two parallel dipole transition moments) can be achieved in such a system. Interference-assisted population trapping, population inversions, and probe gain at one component of the Autler-Townes spectrum are predicted for certain cavity resonant frequencies.

The model consists of a Λ-type three-level atom with the ground sublevels $|0\rangle$ and $|1\rangle$, with a level splitting $\omega_{10}=E_1-E_0$, coupled by the single-mode cavity field to the excited level $|2\rangle$. Direct transitions between the ground doublet $|0\rangle$ and $|1\rangle$ are dipole forbidden. The master equation for the total density matrix operator ρ_T in the frame rotating with the average atomic transition frequency $\omega_0=(\omega_{20}+\omega_{21})/2$ takes the form

$$\dot{\rho}_T=-i[H_A+H_C+H_I,\rho_T]+\mathcal{L}\rho_T, \tag{1}$$

with

$$H_A=\frac{\omega_{10}}{2}(A_{11}-A_{00}), \tag{2}$$

$$H_C=\delta a^\dagger a, \tag{3}$$

$$H_I=i(g_1A_{12}+g_0A_{02})a^\dagger-\text{H.c.}, \tag{4}$$

$$\mathcal{L}\rho_T=\kappa(N+1)(2a\rho_Ta^\dagger-a^\dagger a\rho_T-\rho_Ta^\dagger a)+\kappa N(2a^\dagger\rho_Ta-aa^\dagger\rho_T-\rho_Taa^\dagger), \tag{5}$$

where H_C, H_A, and H_I are the unperturbed cavity, the unperturbed atom, and the cavity-atom interaction Hamiltonians, respectively, while $\mathcal{L}\rho_T$ describes damping of the cavity field by the continuum electromagnetic modes at finite temperature, characterized by the decay constant κ and the mean number of thermal photons *N*; *a* and $a^\dagger$ are the photon annihilation and creation operators of the cavity mode, and $A_{ij}=|i\rangle\langle j|$ is the atomic population (the dipole transition) operator for $i=j$ $(i\neq j)$; $\delta=\omega_C-\omega_0$ is the cavity detuning from the average atomic transition frequency, and $g_i=\mathbf{e}_\lambda\cdot\mathbf{d}_{i2}\sqrt{\hbar\omega_C/2\epsilon_0V}$ $(i=0,1)$ is the atom-cavity coupling constant with $\mathbf{d}_{i2}$, the dipole moment of the atomic transition from $|2\rangle$ to $|i\rangle$, $\mathbf{e}_\lambda$, the polarization of the cavity mode, and *V*, the volume of the system. In the remainder of this work

*Electronic address: peng.zhou@physics.gatech.edu

we assume that the polarization of the cavity field is preselected, i.e., the polarization index λ is fixed to one of two possible directions.

In this paper we are interested in the bad cavity limit $\kappa \gg g_i$, that is, the atom-cavity coupling is weak and the cavity has a low Q so that the cavity field decay dominates. For simplicity, we here assume that the rate γ of spontaneous emission of the atom to background modes other than the privileged cavity mode is negligible small. These conditions may be easily achieved with current experimental techniques. For example, in a recent cavity QED experiment with squeezed light carried out in Kimble's group, the atomic and cavity parameters were set to $\{\kappa,g,\gamma\} = 2\pi\{200,40,2.5\}$ MHz [14]. Agarwal, Lange, and Walther have recently developed a theory based on the bad cavity limit and without accounting for the atomic decay to the background ($\gamma=0$), which perfectly describes their experimental observations [15]. In fact, the early cavity QED experiments were mostly conducted in the bad cavity (weak coupling) regime [14–16].

In the bad cavity limit, the cavity field response to the continuum modes is much faster than that produced by its interaction with the atom, so that the atom always experiences the cavity mode in the state induced by the thermal reservoir. Thus one can adiabatically eliminate the cavity-mode variables, giving rise to a master equation for the atomic variables only [15,17], which takes the form

$$\begin{aligned}\dot{\rho} = & -i[H_A,\rho]+\{F(-\omega_{10})(N+1)[|g_0|^2(A_{02}\rho A_{20}-A_{22}\rho) \\ & + g_0 g_1^* A_{02}\rho A_{21}]+F(\omega_{10})(N+1)[|g_1|^2(A_{12}\rho A_{21} \\ & - A_{22}\rho)+g_0^* g_1 A_{12}\rho A_{20}]+F(-\omega_{10})N \\ & \times[|g_0|^2(A_{20}\rho A_{02}-\rho A_{00})+g_0 g_1^* \\ & \times(A_{21}\rho A_{02}-\rho A_{01})]+F(\omega_{10})N[|g_1|^2(A_{21}\rho A_{12}-\rho A_{11}) \\ & + g_0^* g_1(A_{20}\rho A_{12}-\rho A_{10})]+\text{H.c.}\}, \end{aligned} \tag{6}$$

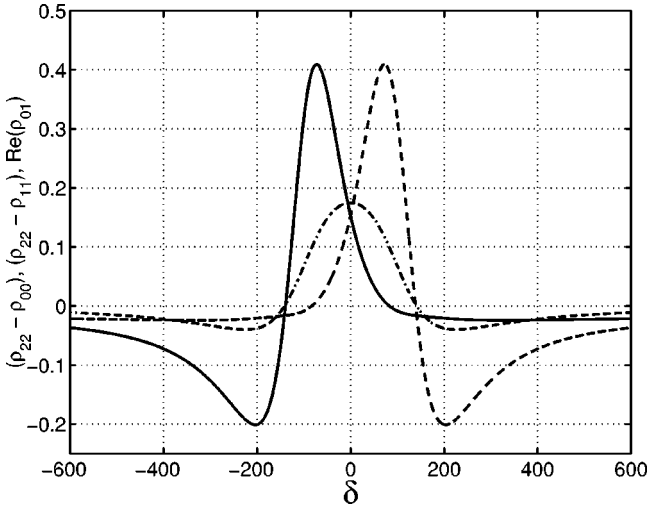

FIG. 1. The steady-state population differences and coherence vs the cavity detuning for $g_0=g_1=10$, $\kappa=100$, $\omega_{10}=200$, and $N=20$. The solid, dashed, and dot-dashed lines represent $(\rho_{22}-\rho_{00})$, $(\rho_{22}-\rho_{11})$, and $\text{Re}(\rho_{01})$, respectively.

where $F(\pm\omega_{10})=[\kappa+i(\delta\pm\omega_{10}/2)]^{-1}$.

Obviously, Eq. (6) describes the cavity-induced atomic decay into the cavity mode. The real part of $F(\pm\omega_{10})|g_i|^2$ represents the cavity-induced decay rate of the atomic excited level $|2\rangle$ to the ground level $|i\rangle$, $(i=0,1)$, while the imaginary part is associated with the frequency shift of the atomic level resulting from the interaction with the thermal field in the detuned cavity. The other terms $F(\pm\omega_{10})g_i g_j^*$, $(i\neq j)$, however, represent the cavity-induced correlated transitions of the atom, i.e., as the atom emits a photon from the excited level $|2\rangle$ to one of the ground sublevels, say $|0\rangle$, for example, it drives an absorption of the same photon on a different transition, $|1\rangle\rightarrow|2\rangle$, and vice versa, which give rise to the effect of quantum interference.

The effect of quantum interference is very sensitive to the orientations of the atomic dipoles and the polarization of the cavity mode. For instance, if the cavity-field polarization is not preselected, as in free space, one must replace $g_i g_j^*$ by the sum over the two possible polarization directions, giving $\Sigma_\lambda g_i g_j^* \propto \mathbf{d}_{i2}\cdot\mathbf{d}_{j2}^*$ [10]. Therefore, only nonorthogonal dipole transitions lead to nonzero contributions, and the maximal interference effect occurs with the two dipoles parallel. As pointed out in Refs. [2,6,10,11], however, it is questionable whether there is a isolated atomic system with parallel dipoles. Otherwise, if the polarization of the cavity mode is fixed, say $\mathbf{e}_\lambda=\mathbf{e}_x$, the polarization direction along the x-quantization axis, then $g_i g_j^* \propto (\mathbf{d}_{i2})_x(\mathbf{d}_{j2}^*)_x$, which is nonvanishing, regardless of the orientation of the atomic dipole matrix elements. Actually, by selecting the cavity polarization, we can in some cases even engineer a system with two parallel or anti-parallel dipole moments. For example, for an atom with Zeeman ground states with a $|j,m=0\rangle \leftrightarrow |j-1,m=\pm1\rangle$ transition, if we preselected the cavity polarization to the x-quantization axis, we will achieve a scheme with two parallel dipole moments, whereas if the cavity polarization is preselected to the y-quantization axis, we will have a system with two antiparallel dipole moments.

It is apparent that if $\kappa \gg \delta,\omega_{10}$, the frequency shifts are negligibly small. Moreover, if we define the cavity-induced decay rates of the excited level to the ground sublevels as $\gamma_0=\kappa|g_0|^2/[\kappa^2+(\delta-\omega_{10})^2]\simeq|g_0|^2/\kappa$ and $\gamma_1=\kappa|g_1|^2/[\kappa^2+(\delta+\omega_{10})^2]\simeq|g_1|^2/\kappa$, the master equation (6) then reduces to the approximate form

$$\begin{aligned}\dot{\rho} \simeq & -i[H_A,\rho]+\gamma_0(N+1)(2A_{02}\rho A_{20}-A_{22}\rho-\rho A_{22}) \\ & + \gamma_0 N(2A_{20}\rho A_{02}-A_{00}\rho-\rho A_{00})+\gamma_1(N+1) \\ & \times(2A_{12}\rho A_{21}-A_{22}\rho-\rho A_{22})+\gamma_1 N(2A_{21}\rho A_{12}-A_{11}\rho \\ & - \rho A_{11})+2\sqrt{\gamma_0\gamma_1}(N+1)A_{12}\rho A_{20} \\ & + \sqrt{\gamma_0\gamma_1}N(2A_{21}\rho A_{02}-A_{01}\rho-\rho A_{01}) \\ & + 2\sqrt{\gamma_0\gamma_1}(N+1)A_{02}\rho A_{21}+\sqrt{\gamma_0\gamma_1}N \\ & \times(2A_{20}\rho A_{12}-A_{10}\rho-\rho A_{10}). \end{aligned} \tag{7}$$

This equation is same as that of a Λ-type three-level atom with two parallel transition matrix elements in free space [9]. In other words, the maximal effect of quantum interference in a Λ-type atom can be achieved in a cavity with a preselected polarization. Furthermore, transforming Eq. (7) into the basis $\{|2\rangle, |S\rangle = (\sqrt{\gamma_0}|0\rangle + \sqrt{\gamma_1}|1\rangle)/\sqrt{\gamma_0+\gamma_1}, |A\rangle = (\sqrt{\gamma_0}|1\rangle - \sqrt{\gamma_1}|0\rangle)/\sqrt{\gamma_0+\gamma_1}\}$, shows that the cavity mode only couples to the states $|S\rangle$ and $|2\rangle$ with a cavity-induced decay rate of $(\gamma_0+\gamma_1)$, and the asymmetric state $|A\rangle$ is decoupled from the excited state $|2\rangle$. Interestingly, in the case of degenerate ground states ($\omega_{10}=0$), the steady-state solution is highly dependent upon initial conditions of the atom. For example, if the atom is initially in the asymmetric state $|A\rangle$, it will stay in the state forever, i.e., $|A\rangle$ is a complete trapped state, whereas the steady-state populations are, respectively, $\rho_{22}=N/(2N+1)$, $\rho_{SS}=(N+1)/(2N+1)$, and $\rho_{AA}=0$, if the atom is initially in either the symmetric state $|S\rangle$ or the excited state $|2\rangle$. Otherwise, for the atom initially in one of the ground doublet, $\rho_{22}=N/(4N+2)$, $\rho_{SS}=(N+1)/(4N+2)$, and $\rho_{AA}=1/2$, where a half population is trapped in the state $|A\rangle$. It is evident that the existence of the population trapped state and the dependence of the steady-state population on the initial atomic states originate from the cavity induced quantum interference.

Our numerical calculations show no trapped state at all in the nondegenerate case ($\omega_{10}\neq 0$). Nevertheless, the cavity-induced quantum interference between the two transition paths $|0\rangle\leftrightarrow|2\rangle$ and $|1\rangle\leftrightarrow|2\rangle$ gives rise to the steady-state population inversions and coherence, as shown in Fig. 1, where $\omega_{10}=2\kappa=200$, $N=20$, and $g_0=g_1=10$ are taken. The steady-state populations and coherence are highly dependent on the cavity frequency. The coherence is symmetric with the cavity detuning and reaches the maximum value at $\delta=0$, while the population differences are asymmetric. Furthermore, the population inversions may be achieved for certain cavity frequency. For example, if the cavity frequency is tuned to $-139.2<\delta<82.3$, the population is inverted between the excited level $|2\rangle$ and the ground sublevel $|0\rangle$ (i.e., $\rho_{22}>\rho_{00}$), whereas $\rho_{22}>\rho_{11}$ in the region of $-82.3<\delta<139.2$. It is clear that $\rho_{22}>\rho_{11}>\rho_{00}$ is achieved in the region of $-139.2<\delta<0$. The steady-state population inversions and nonzero coherence manifests the cavity-induced quantum interference [18].

Now we investigate the effects of cavity-induced interference on the Autler-Townes spectrum $A(\omega)$, by illuminating a weak, frequency-tunable probe field on such a system, which can be calculated from the master equation (6), with the help of the quantum regression theorem:

$$A(\omega)=\frac{2}{\kappa}\mathrm{Re}\left\{\frac{[|g_1|^2a_{12}-g_0g_1^*(a_{11}+i\omega)]\rho_{10}+[|g_0|^2a_{21}-g_0^*g_1(a_{22}+i\omega)]\rho_{01}}{(a_{11}+i\omega)(a_{22}+i\omega)-a_{12}a_{21}}\right\}$$
$$+\frac{2}{\kappa}\mathrm{Re}\left\{\frac{[g_0g_1^*a_{21}-|g_1|^2(a_{22}+i\omega)](\rho_{11}-\rho_{22})+[g_0^*g_1a_{12}-|g_0|^2(a_{11}+i\omega)](\rho_{00}-\rho_{22})}{(a_{11}+i\omega)(a_{22}+i\omega)-a_{12}a_{21}}\right\}, \tag{8}$$

where ρ_{01},ρ_{10} and $\rho_{00},\rho_{11},\rho_{22}$ are the steady coherence and populations of the atom, respecticely, and

$$\begin{aligned}
a_{11}&=-F(\omega_{10})|g_1|^2(2N+1)-F(-\omega_{10})|g_0|^2(N+1)\\
&\quad+\tfrac{1}{2}i\omega_{10},\\
a_{12}&=-F(-\omega_{10})g_0g_1^*N,\\
a_{21}&=-F(\omega_{10})g_0^*g_1N,\\
a_{22}&=-F(\omega_{10})|g_1|^2(N+1)-F(-\omega_{10})|g_0|^2(2N+1)\\
&\quad-\tfrac{1}{2}i\omega_{10}.
\end{aligned} \tag{9}$$

One may predict that in the absence of the cavity-induced interference (i.e., no cross transition associated with $g_0g_1^*$ and $g_1g_0^*$ is taken into account), two transition paths $|0\rangle\leftrightarrow|2\rangle$ and $|1\rangle\leftrightarrow|2\rangle$ are *independent*, which respectively lead to the higher- and lower-frequency sidebands of the absorption doublet with respective linewidths $\gamma_0(2N+1)+\gamma_1(N+1)$ and $\gamma_0(N+1)+\gamma_1(2N+1)$. Whereas, the spectral features may be dramatically modified in the presence of the cavity-induced interference. Here we only concentrate on the case $\omega_{10}\sim 2\kappa \gg \gamma_0,\gamma_1,N$, so that the doublet is well resolved. See, for example, in Fig. 2 where $\omega_{10}=2\kappa=200$, $N=20$, $g_0=g_1=10$ and different cavity detunings are taken, in which the solid (dashed) lines represent the spectrum in the presence (absence) of the cavity induced interference. It is clearly shown that when the cavity is resonant with the average frequency of the atomic transitions $\delta=0$, the interference widens and strengthens the absorption doublet, which is symmetric [Fig. 2(a)]. Otherwise, it is asymmetric. Rather surprisingly, probe gain may occur at either the lower- or the higher-frequency sideband, e.g., the probe field is amplified at the lower-frequency sideband for $\delta=50$ and 100, while at the other sideband for $\delta=200$, see in Figs. 2(b)–2(d), for instance. When the cavity detuning is much larger than the ground sublevel splitting and the cavity linewidth $\delta\gg\omega_{10},2\kappa$, the effect of the cavity induced interference is negligibly small so that the absorption spectrum is virtually same as that without interference (we show no figure here).

It is well known that the probe absorption of multilevel atoms is attributed to population difference between two dipole transition levels and coherence between two dipole forbidden levels, see, for instance, in Eq. (8), and either the

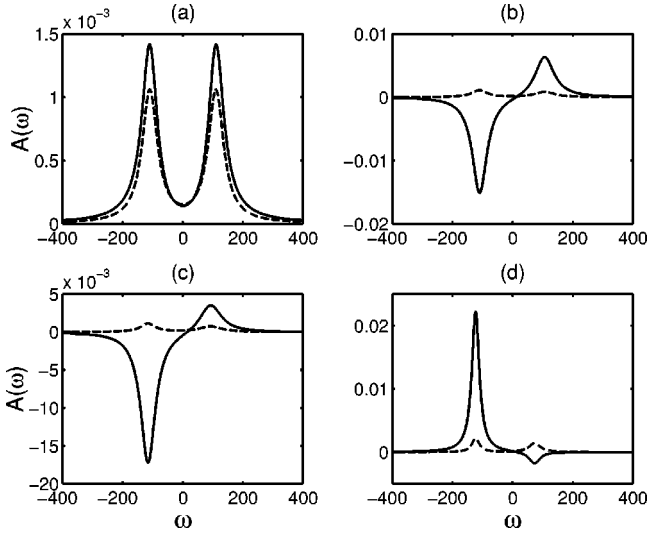

FIG. 2. Absorption spectrum $A(\omega)$ vs the scaled frequency $\omega=(\omega_p-\omega_0)$, where ω_p is the frequency of the probe field, for $g_0=g_1=10$, $\kappa=100$, $\omega_{10}=200$, $N=20$, and $\delta=0$, 50, 100, 200 in (a)–(d), respectively. The solid curves represent the spectrum in the presence of the cavity-induced interference, while the dashed curves are the spectrum in the absence of the interference.

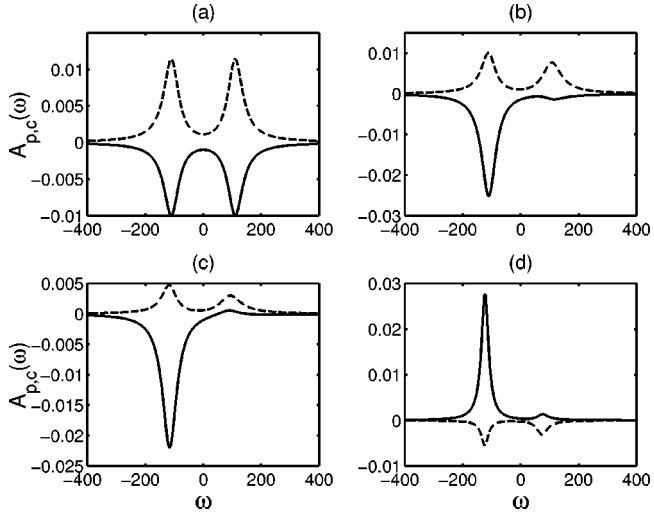

FIG. 3. Different contributions to the absorption spectrum, for $g_1=g_2=10$, $\kappa=100$, $\omega_{21}=200$, $N=20$, and $\delta=0$, 50, 100, 200 in (a)–(d), respectively. The dashed curves represent the contributions of the coherences, while the solid curves are the ones of the population differences.

inverted populations or the coherence can lead to probe gain. As demonstrated in Fig. 1, the population between the two transition levels $|2\rangle$ and $|1\rangle$ is inverted in the region of $-82.3<\delta<139.2$. Therefore, the gain at the lower-frequency sideband stems from the cavity-induced steady-state population inversion between $|2\rangle$ and $|1\rangle$ for $\delta=50$ and 100, whereas the cavity-induced coherence between the two dipole-forbidden excited sublevels $|0\rangle$ and $|1\rangle$ must be the origin of the gain at the higher-frequency one in the case $\delta=200$.

To further explore the origin of the probe gain, we separate the Autler-Townes spectrum into two parts, in which one corresponds to the contribution of the coherence, represented by the first part of the right-hand side (RHS) of Eq. (8) and the dashed curves in Fig. 3, while the other results from the populations, the second part of the RHS of Eq. (8) and the solid lines in Fig. 3. We have assumed that $g_1=g_2=10$, $\kappa=100$, $\omega_{10}=200$, $N=20$, and various cavity frequencies in Fig. 3. It is obvious that when $\delta=0$, 50, and 100, the contributions of the populations to the spectrum are of amplification of the probe beam, due to the population inversions, whereas the coherence make positive contributions (probe absorption), see, for example, Figs. 3(a)–3(c). One can also see that the spectral component resulting from the populations is symmetric only when $\delta=0$, otherwise, it has different values at the lower and higher frequency sidebands, which are proportional to $(\rho_{22}-\rho_{11})$ and $(\rho_{22}-\rho_{00})$, respectively. As shown in Fig. 1, if the cavity detuning is zero, then $(\rho_{22}-\rho_{11})=(\rho_{22}-\rho_{00})$, whereas $(\rho_{22}-\rho_{11})>(\rho_{22}-\rho_{00})$ for $\delta=50$ and 100. As a result, the lower frequency sideband is deeper than the other in the cases $\delta=50$ and $\delta=100$. The total spectrum may therefore exhibit probe gain at the lower frequency sideband at these cavity frequencies. See, for example, Figs. 3(c) and 3(d). However, when $\delta=200$, the situation is reversed: the coherence gives rise to probe gain, while the populations lead to probe absorption at both the sidebands. The net probe gain occurs at the higher frequency sideband, which is purely attributable to the cavity-induced steady-state atomic coherence. We can anticipate the similar results occur with $\delta<0$, but the higher-frequency gain is due to the population inversion, while the lower-frequency one is attributed to the nonzero coherence.

With an ensemble of many atoms inside the cavity, cooperative effects may lead to larger coherence and population inversions, in turn, a larger probe gain. According to the linear response theory, the absorption coefficient $\alpha=\alpha_0\mathrm{Im}[\rho_{21}(\omega_p)+\rho_{20}(\omega_p)]/\mathcal{E}_p$, where $\mathcal{E}_p$ is the amplitude of the weak probe beam, $\rho_{21}(\omega_p)$, $\rho_{20}(\omega_p)$ are associated with atomic complex polarizations at the probe frequency ω_p, and α_0 is proportional to the number density of atoms [19]. One can therefore expect that the more atoms are injected into the cavity, the larger gain (or absorption) may be produced.

In summary, we have shown that maximal quantum interference can be practically achieved in a Λ-type atom coupled to a single-mode, frequency-tunable cavity field at finite temperature, with a preselected polarization in the bad cavity limit. The cavity-induced interference may give rise to the population trapping and inversions, and the probe gain at either sideband of the Autler-Townes doublet, depending upon the cavity resonant frequency, the ground level splitting, and the mean number of thermal photons. The gain occurring at different sidebands has the various origin: in the case of $\delta>0$, the higher-frequency gain is due to the nonzero coherence, while the lower-frequency one is attributed to the population inversion. As shown in Refs. [3,8,13], an applied laser coupling to multilevel atoms may result in the steady-state coherence and population inversions. We here present another scheme whereby they can be generated by the cavity-induced interference.

We should emphasize that there are no special restrictions on the atomic dipole moments in our system, as long as the polarization of the cavity field is preselected and the effects of the cavity-induced interference occur over ranges of the parameters, and are profound when the ground level splitting is the same order of the cavity linewidth and the mean number of thermal photons $N \gg 1$, which should be applicable to a wide range of atomic species. In this sense, our study may provide a way to generate new short-wavelength lasers (i.e., probe gain at the higher frequency sideband).

This work was partially done at the Department of Applied Mathematics and Theoretical Physics, The Queen's University of Belfast. I would like to thank Z. Ficek and S. Swain for helpful conversations.

[1] E. Arimondo, in *Progress in Optics*, XXXV, edited by E. Wolf (North Holland, Amsterdam, 1996), p. 257; M.O. Scully and S.Y. Zhu, Science **281**, 1973 (1998).

[2] S.E. Harris, Phys. Rev. Lett. **62**, 1033 (1989); S.E. Harris and J.J. Macklin, Phys. Rev. A **40**, R4135 (1989); A. Imamoglu, *ibid.* **40**, R2835 (1989); P. Zhou and S. Swain, Phys. Rev. Lett. **78**, 832 (1997); J. Opt. Soc. Am. B **15**, 2583 (1998).

[3] K.J. Boller, A. Imamoglu, and S.E. Harris, Phys. Rev. Lett. **66**, 2593 (1991); M. Xiao *et al.*, *ibid.* **74**, 666 (1995).

[4] M.O. Scully, Phys. Rev. Lett. **67**, 1855 (1991); A.S. Zibrov, *et al.*, *ibid.* **76**, 3935 (1996).

[5] H.R. Xia, C.Y. Ye, and S.Y. Zhu, Phys. Rev. Lett. **77**, 1032 (1996).

[6] D.A. Cardimona, M.G. Raymer, and C.R. Stroud Jr., J. Phys. B **15**, 65 (1982); S.Y. Zhu and M.O. Scully, Phys. Rev. Lett. **76**, 388 (1996); E. Paspalakis and P.L. Knight, *ibid.* **81**, 293 (1998).

[7] P. Zhou and S. Swain, Phys. Rev. Lett. **77**, 3995 (1996); Phys. Rev. A **56**, 3011 (1997); C.H. Keitel, Phys. Rev. Lett. **83**, 1307 (1999).

[8] L.M. Narducci *et al.*, Phys. Rev. A **42**, 1630 (1990); A.S. Manka *et al.*, *ibid.* **43**, 3748 (1991); D.J. Gauthier, Y. Zhu, and T.W. Mossberg, Phys. Rev. Lett. **66**, 2460 (1991); M.D. Lukin *et al.*, *ibid.* **79**, 2959 (1997); **81**, 2675 (1998); **82**, 1847 (1999).

[9] J. Javanainen, Europhys. Lett. **17**, 407 (1992); S. Menon and G.S. Agarwal, Phys. Rev. A **57**, 4014 (1998).

[10] J.E. Field, Phys. Rev. A **47**, 5064 (1993); A.K. Patnaik and G.S. Agarwal, *ibid.* **59**, 3015 (1999); P. Zhou, Opt. Commun. **178**, 141 (2000); P Zhou and S. Swain, *ibid.* **179**, 267 (2000); G.S. Agarwal, Phys. Rev. Lett. **84**, 5500 (2000).

[11] P.R. Berman, Phys. Rev. A **58**, 4886 (1998).

[12] J. Wang, H.M. Wiseman, and Z. Ficek, Phys. Rev. A **62**, 013818 (2000).

[13] M.O. Scully, S.Y. Zhu, and A. Gavrielides, Phys. Rev. Lett. **62**, 2813 (1989). M. Fleischauer *et al.*, Opt. Commun. **94**, 599 (1992); S.Y. Zhu, L.M. Narducci, and M.O. Scully, Phys. Rev. A **52**, 4791 (1995); G.S. Agarwal, *ibid.* **54**, R3734 (1996).

[14] H. J. Kimble *et al.*, in *Atomic Physics 14*, edited by D. J. Wineland, C. E. Wieman, and S. J. Smith (AIP, New York, 1995).

[15] W. Lange and H. Walther, Phys. Rev. A **48**, 4551 (1993); G.S. Agarwal, W. Lange, and H. Walther, *ibid.* **48**, 4555 (1993).

[16] D. Kleppner, Phys. Rev. Lett. **47**, 233 (1981); P. Goy, J.M. Raimond, M. Gross, and S. Haroche, *ibid.* **50**, 1903 (1983); R.G. Hulet, E.S. Hilfer, and D. Kleppner, *ibid.* **55**, 2137 (1985); D.J. Heinzen, J.J. Childs, J.E. Thomas, and M.S. Feld, *ibid.* **58**, 1320 (1987); Y. Zhu, A. Lezama, and T.W. Mossberg, *ibid.* **61**, 1946 (1988); For recent reviews, see, for example, *Cavity Quantum Electrodynamics*, edited by P. R. Berman (Academic, P London, 1994).

[17] P. Zhou and S. Swain, Phys. Rev. A **58**, 1515 (1998).

[18] Noting that in the steady state $\rho_{00}=\rho_{11}=(N+1)/(3N+2)$, $\rho_{22}=N/(3N+2)$, and $\rho_{01}=0$ in the absence of interference.

[19] P. Meystre and M. Sargent III, *Elements of Quantum Optics* (Springer, Berlin, 1991).